78-1183

Viscous Drag Computation for Axisymmetric Bodies at High Reynolds Numbers

M. Fouad Zedan* and Charles Dalton†
University of Houston, Houston, Texas

A critical comparison has been made between the drag characteristics of a number of the best available axisymmetric body shapes using a numerical drag calculation scheme. Assuming a turbulent boundary layer over most of the body surface at $R_{\forall} = 10^8$, the study shows that all profiles have almost equal drag coefficients when referenced to the two-third power of the body volume. However, based on the projected area, several laminar bodies were found to have substantially lower drag coefficients. Transition studies indicate that a short run of laminar boundary-layer flow, X/L to about 0.2, may be expected by moving the maximum thickness forward and carefully designing the nose shape through the inverse method. At $R_{\forall} = 5 \times 10^7$, all bodies, with the exception of the Shark and F-57, have the same transition and drag characteristics. The study also shows that the F-57 shape has a much higher transition risk than the Shark in the range $0.08 \leq X/L \leq 0.13$. Otherwise, the F-57 shape has better performance. Increasing the flow acceleration in this range is expected to eliminate the transition possibility and the superiority of the F-57 profile becomes undisputed.

Introduction

STIMULATED by the interest in high-performance undersea vehicles, the problem of the design of low-drag axisymmetric body shapes has recently received considerable attention in the literature. Currently, this attention is enhanced by the energy crisis and the need for the development of some means for long-distance handling of large, bulky cargo. Recent studies[1] showed that large airships 800-1000 ft in length can provide an efficient means for that purpose. The Reynolds number, $R_{\forall}$ $(= U_\infty \forall^{1/3}/\nu)$ for such bodies is in the order of 10^8. The aerodynamic design of the airship is now about 40 years old. The tremendous progress in the understanding of the flow physics and in the boundary-layer prediction around aero/hydrodynamic bodies achieved during this period should be utilized in the design of the proposed airships. Other applications of low-drag body design at high Reynolds numbers are torpedoes and submarines, deeply submerged and moving at high speed. In fact, most of the low-drag studies were carried out for axisymmetric underwater vehicle design. These resulted in the development of a number of new profiles which have lower drag than the conventional shapes in the volume Reynolds number range 5×10^6-10^7.

While there are different means for drag reduction, such as boundary-layer control by polymer injection or by suction, body shaping is clearly the most economical means. Parsons and Goodson[2] made a very significant contribution in this direction; however, the highest $R_{\forall}$ investigated was 5×10^7.

In the present study, we are concerned with drag due to fluid friction at $R_{\forall} = 5 \times 10^7$-$10^8$, where there is a clear lack of theoretical studies and experimental investigations are impractical. The first phase in our program, reported herein, is a comparison between the drag characteristics of a number of the best available profiles for high Reynolds number application. The motivation behind this is twofold: 1) to determine the best available body shape for the design of airships and high-speed underwater vehicles; 2) to study how different surface velocity distributions affect the drag. This may lead to some information about the characteristics (or at least establish trends) of the surface velocity distribution of low-drag shapes. These characteristics are needed in order to make use of the newly developed inverse problem solutions by Bristow[3] and Zedan and Dalton.[4,5] This has, in principle, the potential of developing new profiles or, at least, improving the currently best available shape.

Since the primary function of most of the applications of this study is to carry a given payload, it seems logical to use the one-third power of the volume as the characteristic length. Therefore, this investigation is carried out for a given $R_{\forall}$. Two values, 10^8 and 5×10^7, were chosen. The first is representative of large airships and small submarines, while the second represents the case of high-speed, large torpedoes and small airships.

II. Previous Studies

In 1950, Gertler[6] dealt with the problem of low-drag body design experimentally. Using five parameters to characterize the body shape, he built 24 models of different shapes, known as "Series 58." The overall drag was measured, but not the boundary-layer characteristics. The bodies were tested by towing through water at different speeds. Gertler's study was carried out for submarine design ($R_{\forall} \simeq 3 \times 10^8$). Since the test Reynolds number was approximately 5×10^6, the boundary layer was tripped at 5% of the body length to simulate the prototype case. Parsons and Goodson[2] criticized Gertler's study from the viewpoint that a one-at-a-time parameter perturbation about a parent model is not an optimization procedure in the true sense. Consequently, Gertler's study indicated a "best shape" and not an "optimum shape." However, the sizable amount of experimental data of this study, which has been described by Hess[11] as highly accurate, has served over the years as test cases for computational schemes in an area where experimental results are rare.

In another experimental study by Carmichael[12] in 1966, a new low-drag body emerged through shape manipulation. Carmichael showed that by reducing the fineness ratio (F.R.), the surface area and, consequently, the drag is reduced either for constant frontal area or constant volume application. Then, by proper hull shaping in analogy with laminar airfoils,

Presented as Paper 78-1183 at the AIAA 11th Fluid and Plasma Dynamics Conference, Seattle, Wash., July 10-12, 1978; submitted July 25, 1978.

Index categories: Hydrodynamics; Aerodynamics; Lighter-than-Airships.

*Currently Design Engineer, Offshore Structures Dept. (R&D), Brown & Root, Inc., Houston, Texas.

†Associate Professor, Dept. of Mechanical Engineering.

a body of F.R. = 3.33 was deduced from the NACA-66 airfoil series. This tailboomed body (dubbed the "Dolphin") was tested extensively in the Pacific Ocean using gravity power. The Dolphin achieved over 60% drag reduction compared to a conventional torpedo of equal volume for $R_L = 2\times10^7$ to 3×10^7. Transition length Reynolds numbers of 1.4×10^7 to 1.8×10^7 were deduced by comparison of experiment with theory. Clearly, low fineness ratio and proper shape can provide strong flow acceleration in the front part of the body. This serves to keep the boundary layer laminar over an appreciable distance. This proved to be a very effective technique in viscous drag reduction.

Also in 1966, Hertel[13] investigated the problem of integration of lifing fans into the VTOL subsonic aircraft structure to avoid more drag due to additional surfaces. Hertel considered the shapes of the fast-swimming animals. He showed that for bodies of revolution of profile identical to the NACA two-dimensional laminar shapes (similar to the Tunny), the substantial pressure drop ceases at $X/L = 0.1$ compared to 0.6 for the two-dimensional profile. Thus, this class of bodies is not expected to provide the proper pressure gradient for the boundary layer to remain laminar in contrast to bodies with a parabolic nose, such as the Dolphin‡ and the Shark. Hertel developed a new fuselage shape characterized by large thickness (22%), sharp nose, and rounded tail. Transition calculations for this body (called Shark 1) indicated that the laminar boundary layer (LBL) can survive up to $X/L = 0.35$ at $R_L = 10^8$, due to the strong flow acceleration which extends to $X/L = 0.4$. This results in a considerable drag reduction. If one considers the drag coefficient based on $\nabla^{2/3}$, this body's high geometrical efficiency (due to small F.R.) makes it more promising.

Parsons and Goodson[2] made a significant contribution by successfully developing a computer-oriented optimization procedure together with a drag calculation scheme for the automatic synthesis of minimum drag hull shapes for specified R_∇. The closed-body shape was described by five parameters and the tailboomed body by eight. These parameters were determined from the optimization procedure by the condition of minimum drag. The study produced a number of suboptimum body shapes at different R_∇ in the range 5×10^6 to 5×10^7. At $R_\nabla = 10^7$, a tailboomed body with a drag coefficient one-third below the Dolphin of Carmichael[12] was developed. This body, dubbed X-35, is well-documented in Ref. 14. At $R_\nabla = 5\times10^7$, two different body shapes (F-57 and F2-49) with approximately the same drag, were obtained. In all these laminar bodies, the LBL is sustained over as much surface as possible while keeping the body at an appropriate geometry to avoid TBL separation. For turbulent design, the transition point was fixed at $X/L = 0.05$. The optimization procedure at $R_\nabla = 5\times10^6$ indicated that the drag coefficient based on $\nabla^{2/3}$ varies little over fairly wide variations in body shape (or parameters). The best turbulent body design, called I-36 by Parsons and Goodson, showed no significant improvement over model 4165 of Gertler.[6]

Recently, two theoretical studies were carried out by Hess[11] and Myring.[15] The intent was to develop low-drag bodies for applications where the boundary layer is expected to be turbulent over most of the body. Myring studied the effect of body shape, which is described by five parameters, on the drag coefficient C_{DS}, based on the surface area. The transition location was fixed at $X/L = 0.03$ with $R_L = 10^7$. The boundary-layer calculation scheme was based on viscous-inviscid flow interaction, in which the outer potential flow is modified by boundary-layer growth by adding the displacement effect to the body surface in an iterative manner. Varying one parameter at a time, the study showed that changes in the body shape can produce a reduction of as much as 10% in C_{DS} at the same F.R. The low-drag body developed in this study has continuously changing area distribution. As for the effects of R_L and F.R., the results were surprisingly in good agreement with those of the older, unsophisticated study of Young.[16]

Assuming the boundary layer to start turbulent at the nose, Hess[11] developed a simplified integral drag formula and used it to compare the drag performance over a wide variety of bodies. The main conclusion in this study was the insensitivity of $C_{D\nabla}$ to the hull shape. In fact, $C_{D\nabla}$ vs F.R. for prolate spheroids correlates the drag for all "good" (presumably smooth) bodies. The curve has a shallow minimum in the range F.R. = 3-4. Hess suggested boattailing of the spheroids to avoid separation. Another result indicated by the simplified integral formula is that a body which is optimum at one Reynolds number is optimum at all other numbers provided, of course, the boundary layer is turbulent and does not separate. Because of the lack of information about the properties of the velocity distribution of a low-drag shape, Hess found the use of the inverse problem to be limited at that time. However, he tried to use the inverse method to design what he called "cavitation" bodies having extensive regions of constant pressure. Unfortunately, their performance was not much different from prolate spheroids.

III. Flow Model and Computational Scheme

The flow around an axisymmetric body is, in general, highly complex. However, if the Reynolds number is high enough, the flowfield may be divided into a thin layer near the body surface, an irrotational region outside the boundary layer, and a wake (or separated region) aft of the body. The boundary layer starts laminar at the nose, then transition to turbulence is triggered at some location (actually over a region) downstream. If no separation occurs, most of the drag is caused by skin friction along the surface. The skin friction distribution can be computed from the boundary-layer solution.

The drag of an axisymmetric body can be evaluated by either of two methods: integration of the shear stress and surface pressure distributions over the body surface or by consideration of the wake momentum deficit. Cebeci and Smith[17] showed that the former approach is inaccurate. Using an approximate solution for the wake flow, Young[16] was able to relate the drag coefficient to the characteristics of the boundary layer at the tail of the body. A similar formula was later derived by Granville.[18] It has been found that these two methods have almost the same degree of accuracy. In the present work, Young's formula is used and is given by

$$C_D = \left[\frac{4\pi(r_0\theta)}{A}\left(\frac{U}{U_\infty}\right)^{(H+5)/2}\right]_{T.E.} \tag{1}$$

where θ is the momentum thickness defined in a manner appropriate to axisymmetric boundary layers, A is a reference area which is taken equal to (volume)$^{2/3}$ in this study, and $H(=\delta^*/\theta)$ is the boundary-layer shape factor. The definitions of displacement and momentum thickness are

$$\delta^* = \int_0^\delta \left(1-\frac{u}{U}\right)\frac{r}{r_0}\,dn \qquad \theta = \int_0^\delta \frac{u}{U}\left(1-\frac{u}{U}\right)\frac{r}{r_0}\,dn \tag{2}$$

where n, r_0, u, and U are shown in Fig. 1. The relation between these parameters and the corresponding planar ones $(\bar\delta^*, \bar\theta)$ can be derived by assuming a form for the boundary-layer velocity distribution. Cebeci, et al.[19] and Patel[8] have derived such relations for power-law velocity profiles and showed that the difference between corresponding parameters is negligible as long as $r_0/\delta \gg 1$, which is not the situation near the tail. However, some of the boundary-layer calcuation methods use the planar definitions.

‡It should be noted that this Dolphin shape is different from the body developed by Carmichael with the same name.

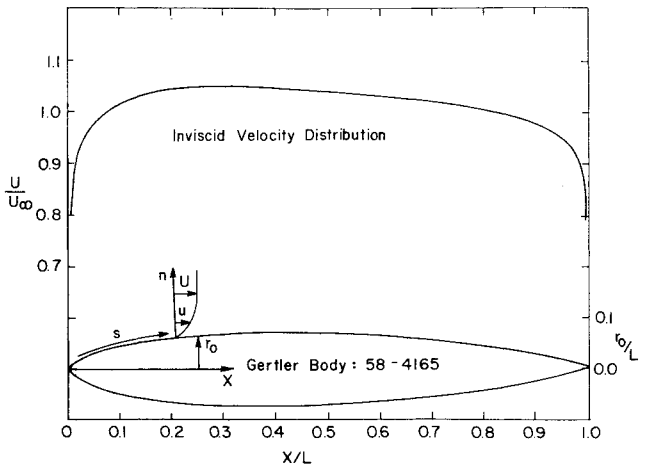

Fig. 1 Profile shape and velocity distribution for Gertler body 58-4165.

Flow Outside the Boundary Layer

To solve the boundary-layer equations, one needs the pressure gradient along the surface. If the assumptions of a thin boundary layer and small streamwise curvature are satisfied, it can be shown that the outside pressure is impressed on the boundary layer by the outer flow; i.e., $\partial P/\partial n \simeq 0$ and $\partial P/\partial s$ can be obtained from the flow outside the boundary layer.[20,7] Assuming irrotational flow, the outside pressure distribution can be obtained from the potential flow velocity distribution via the Bernoulli equation. Hess and Smith[21] showed that the potential flow pressure distribution is in good agreement with the experimental measurements on "pointed" and "blunted" cone-cylinders in axisymmetric unseparated flow. For streamlined bodies with a dominant rear stagnation point, Nakayama and Patel[10] showed good agreement for $X/L \leq 0.9$. The disagreement near the tail is attributed to the strong interaction between the thick boundary layer and the irrotational flow outside it. Parsons and Goodson[2] implied that this difficulty is not encountered for bodies with cusped tails (having an inflection point). Cebeci, et al.[22] used a viscous correction which had a negligible effect everywhere except near the tail. However, instead of the preceding elaborate procedure, they suggested either of two alternatives: replace the rear-stagnation velocity distribution by a linar extrapolation of the inviscid velocity from 95% of the length to the tailing edge or apply the drag formula at an "effective end" of the body. In the present study, however, the potential pressure distribution is used without modification for reasons to be stated later and because some of the previous corrections seemed quite arbitrary.

The potential flow solutions for bodies of revolution are well established. A critical review of these methods is given by Zedan and Dalton.[5] In the present study, we have used the surface singularity method known as the "Douglas-Neumann" method developed at the Douglas Aircraft Company.[21,23] This method proved to be more accurate than our axial singularity method for the direct problem as applied to bodies with an inflection point.[5] However, we have recently resolved the inflection point difficulty and have found the axial singularity method is quite accurate for such bodies.

Boundary-Layer Development

Cebeci, Smith, and Wang[24] developed a numerical method (CS for LBL) to solve the LBL equations in differential form with transverse curvature effects retained. They used a variable-grid, finite-difference scheme for both planar and axisymmetric flows.

Other methods are based on the solution of the boundary-layer equations in integral form. Among these are the methods of Truckenbrodt[25] and an extension of Thwaites' method to axisymmetric flow by Rott and Crabtree.[26] Although these methods are approximate and simple, they yield accurate results, at least as far as boundary-layer growth is concerned. Early in this investigation, the method of Truckenbrodt, which is based on the solution of both the momentum and energy integral equations, was considered. The momentum thickness and shape factor are given by simple quadrature formulas. When these equations were programmed, we encountered numerical difficulties in the calculation of the shape factor. Comparison with the results of the CS method, reported by Parsons, et al.[14] for body X-35, showed very good agreement for θ but not so good for H. For example, setting the laminar separation criterion based on H, the method failed to detect separation at $X/L = 0.7$. Therefore, the method was replaced by Thwaites' method, as presented by Cebeci and Bradshaw[7] for axisymmetric flow. Again, θ is given by the simple quadrature formula

$$\left(\frac{\theta}{L}\right)^2 = \frac{a}{R_L R_0^2 (U/U_\infty)^6} \int_0^{\bar{s}} (U/U_\infty)^5 R_0^2 \mathrm{d}\bar{s} \tag{3}$$

where $R_0 = r_0/L$, $\bar{s} = s/L$, $R_L = U_\infty L/\nu$, $a = 0.45$, and L is the body length. It should be noted that Eq. (3) is identical to the Truckenbrodt equation for θ where $a = 0.441$, and to the Rott and Crabtree equation used by Nakayama and Patel with $a = 0.47$. The shape factor relations are as follows:

$$H = 2.61 - 3.75\lambda + 5.24\lambda^2 \quad \text{for} \quad 0 \leq \lambda \leq 0.1 \tag{4a}$$

$$H = \frac{0.0731}{0.14 + \lambda} + 2.088 \quad \text{for} \quad -0.1 \leq \lambda \leq 0 \tag{4b}$$

with $\lambda = (\theta^2/\nu)(\mathrm{d}U/\mathrm{d}s)$. A program for this method is given by Cebeci and Bradshaw.[7] This program has been modified for the present use to improve the calculation of $\mathrm{d}U/\mathrm{d}s$. A parabolic fit through each three neighboring points was used to find the slope at the middle point. Agreement of the results of this program with the more exact CS method for body X-35 was excellent for both θ and H and laminar separation was detected correctly at $X/L = 0.7$. Therefore, the method was considered satisfactory for the current investigation. The LBL calculations stop whenever laminar separation or transition takes place, whichever comes first.

The prediction of the TBL is generally more difficult than the LBL due to the incomplete understanding of the physics of turbulence. The approach is generally semitheoretical and semiempirical because of the closure problem.[27] However, reasonably good methods relying on some empirical correlations have appeared after the mid-sixties when large computers became available. In the current investigation, the Truckenbrodt TBL method[25] was considered, programmed, and applied to body X-35 as a test case to compare with the results of the more recognized CS, TBL finite-difference method.[24] The agreement for θ was fair but not so good for H. However,if one recognizes that the Truckenbrodt method calculates $\tilde{\theta}$ and not θ and then attempts to calculate θ from $\tilde{\theta}$ using a procedure similar to that of Patel,[8] the agreement is reduced. Therefore, the method was abandoned. Instead, we considered a modern integral method developed by Patel.[8] Patel[28] derived a less restrictive form of the momentum-integral equation for a thick axisymmetric TBL, across which there is a non-negligible pressure variation. Patel[8] later showed that this equation can be reduced to the usual form

$$\frac{\mathrm{d}\theta}{\mathrm{d}s} + (2\theta + \delta^*)\frac{1}{\bar{U}}\frac{\mathrm{d}\bar{U}}{\mathrm{d}s} + \frac{\theta}{r_0}\frac{\mathrm{d}r_0}{\mathrm{d}s} = \frac{1}{2}C_f \tag{5}$$

if use is made of a "hypothetical freestream velocity" distribution $\bar{U}$ instead of the measured (actual) velocity distribution. The hypothetical distribution $\bar{U}$ is the velocity implied by the largest longitudinal pressure gradient (which occurs at the surface) in the boundary layer. Experimental measurements of Patel, et al.[29] showed that $\bar{U}$ becomes increasingly less than the actual velocity U for $X/L > 0.8$. Thus, it appears that using the potential flow velocity (which is less than the actual velocity in the tail region) for $\bar{U}$ in conjunction with Eq. (5) may be a better approximation than trying to use any kind of previously mentioned corrections. The method utilizes the skin friction law of Thompson[30] and an entrainment equation developed for axisymmetric boundary layers. The method is capable of predicting thin as well as thick TBLs. Hess[11] has demonstrated that using this method in the drag algorithm produces results that are surprisingly in much better agreement with the experimental drag for a large number of bodies as compared to the CS method.

Transition Prediction

Transition prediction is difficult to accomplish. While successful stability analysis has been realized by linear theory, the late stages of turbulent transition are highly nonlinear. The transition process, leading to turbulence, is probably among the greatest unresolved problems in the physical sciences. The sensitivity of transition to hard-to-control factors, such as surface roughness, level, and frequency distribution of freestream turbulence, pressure gradient, noise, and system vibrations, produces large scatter in experimental data. This makes even the empirical approach, while it seems to be the only alternative at the present time, rather difficult.

Nakayama and Patel[10] considered four transition criteria: Michel, Granville, Crabtree, and Van Driest and Blumer. Michel's method[19] is not used in this paper because the Reynolds number upper bound of this method is exceeded in the present calculation. The comparison with experimental data of four bodies by Nakayama and Patel did not indicate which method is best. In this work, we incorporated the Crabtree[9] and Van Driest and Blumer[31] criteria into the LBL program. Crabtree correlated the transiton data using the same parameters as those for neutral stability; i.e., $U\theta/\nu$ and $\lambda\ [=(\theta^2/\nu)(dU/ds)]$. Van Driest and Blumer expressed their correlation in terms of $U\delta/\nu$, $\Lambda[=(\delta^2/\nu)(dU/ds)]$ and turbulence intensity. The boundary-layer thickness, δ, is calculated from θ using the Pohlhausen velocity profiles.[7,20]

Once the transition location is determined, the TBL calculation is started using the value of θ predicted by the LBL solution, while H is obtained from the TBL equilibrium relations of Nash.[33,34] Using the velocity U, velocity gradient dU/ds, θ at the transition point and an initial guess of $H = 1.4$, the following set of empirical equations is solved iteratively:

$$\pi = \frac{-2H}{C_f}\frac{\theta}{U}\frac{dU}{ds} \tag{6}$$

$$G = 6.1(\pi + 1.81)^{1/2} - 1.7 \tag{7}$$

$$\left(\frac{2}{C_f}\right)^{1/2} = 5.75\log_{10}(HR_\theta) + 1.5G + \frac{2110}{G^2 + 200} - 14.8 \tag{8}$$

$$H = \frac{1}{1 - G(C_f/2)^{1/2}} \tag{9}$$

IV. Results and Discussion

A. Evaluation of the Current Drag Package

To evaluate the performance of the present calculation scheme, comparison with experimental data is necessary. The test case selected is the drag performance of body number 4165 of the Gertler series 58.[6] The potential flow velocity distribution and the body profile are shown in Fig. 1. Forty-seven surface singularity elements are used. The points describing the body surface (consequently, the elements) are distributed with high intensity in the nose and tail regions according to the method given by Zedan.[32]

For body 4165 with $R_\forall = 5.5 \times 10^6$ ($R_L = 2.588 \times 10^7$), LBL calculations were stopped at the sand roughness (trip) location ($X/L = 0.05$) used by Gertler in his towing tank experiments. The TBL calculations are started at this point and continued to the tail. Figure 2 shows the evolution of the momentum thickness and the shape factor based on both the axisymmetric (θ, H) and planar ($\bar{\theta}, \bar{H}$) definitions. It is obvious that the difference between these definitions becomes more pronounced as the tail is approached. Separation is predicted at $X/L = 0.99$; however, it is neglected since it is so close to the trailing edge where a viscous correcton for the velocity distribution could have eliminated this problem.[19] Young's drag formula [Eq. (1)] has been applied along the surface as $C_{D\forall}(X)$ in a manner similar to that suggested by Parsons and Goodson[2] and Nakayama and Patel.[10] This proved to be quite effective in evaluating the limit as the trailing edge is approached. Figure 3 shows $C_{D\forall}(X)$ compared to the

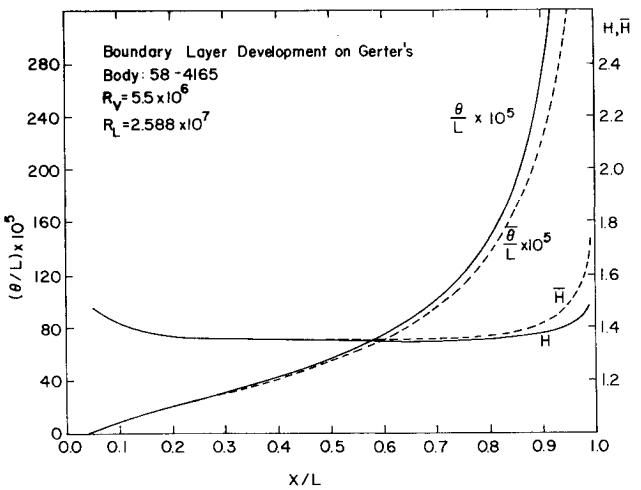

Fig. 2 Boundary-layer development for Gertler body.

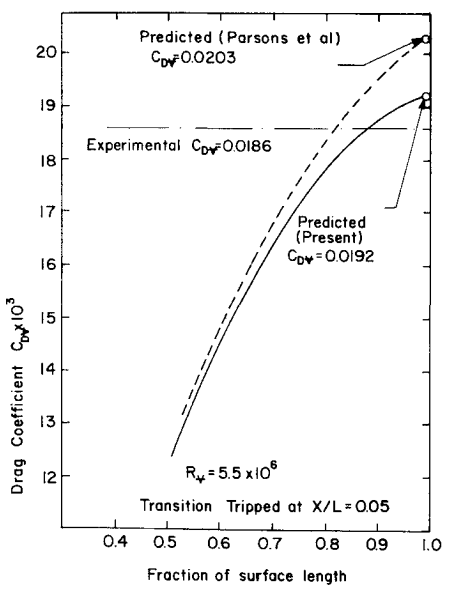

Fig. 3 Drag coefficient prediction comparison for Gertler body.

Table 1 Summary of the geometrical charactertistics and drag calculations at $R_{\forall} = 10^8$ with $X_{tr}/L = 0.034$

Body	Tunny	Dolphin	Shark	F-57	F2-49	Myring	I-36	4165
$L/\forall^{1/3}$	3.6575	4.5292	3.6489	3.7485	3.2193	3.9670	4.6355	4.7059
$S/\forall^{1/3}$	6.3143	6.8366	6.3446	6.1974	5.9014	6.7592	6.9487	7.3126
$A/\forall^{2/3}$	0.4901	0.4878	0.4878	0.6043	0.6645	0.4004	0.4213	0.3550
F. R.	4.6300	5.7470	4.6300	4.2740	3.5000	5.5560	6.3294	7.0000
$10^{-8}R_L$	3.6575	4.5292	3.6489	3.7485	3.2193	3.9670	4.6355	4.7059
$10^{-8}R_A$	0.7001	0.6984	0.6984	0.7774	0.8152	0.6328	0.6491	0.5958
$C_{D\forall}$	0.0130	0.0131	0.0131	0.0131	0.0134	0.0131	0.0128	0.0131
C_{DA}	0.0265	0.0269	0.0268	0.0217	0.0202	0.0327	0.0304	0.0369
C_{DS}	0.00206	0.00192	0.00206	0.00211	0.00227	0.00193	0.00184	0.00179

calculations of Parsons and Goodson.[2] While the experimental C_D is 0.0186, the present scheme predicted 0.0192, a 3.2% error. Parsons and Goodson predicted 0.0203 with 9.1% error using the CS methods for LBLs and TBLs. The relative accuracy of the TBL method used here compared to the CS finite-difference method has been demonstrated for a large number of test cases by Hess.[11] The calculations were repeated for $R_{\forall} = 4.25 \times 10^6 (R_L = 20 \times 10^6)$. The computed $C_{D\forall}$ is 0.02 which corresponds to $C_{DS} = 0.002735$, compared to the experimental value of 0.0027 with an error of 1.3%. Nakayama and Patel[10] predicted a value of 0.00275 with an error of 2.8%. Based on these results, it is obvious that the performance of the present drag package is more than adequate.

B. Different Body Shapes

The body shapes selected for this investigation are shown in Fig. 4. The Tunny and the Dolphin are among the fast-swimming animals considered by Hertel[13] as candidates for low-drag shape. The Shark is the body Hertel developed (and called Shark 1) for $R_L = 10^8$. The F-57 and F2-49 bodies are the suboptimum bodies developed by Parsons and Goodson[2] at $R_{\forall} = 5 \times 10^7$, which is the highest $R_{\forall}$ they investigated. The previously mentioned bodies are regarded as laminar profiles; the other three bodies are the best turbulent designs in the studies of Myring, Parsons and Goodson, and Gertler,

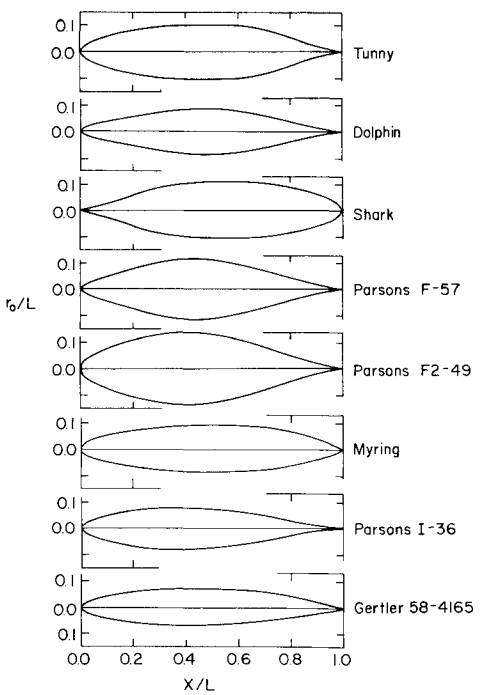

Fig. 4 Body shapes.

respectively. The geometrical characteristics of the eight bodies are given in Table 1. The laminar profiles are characterized by smaller fineness ratios compared to the turbulent profiles. It is worthwhile to mention that there are other "good" laminar designs in the literature, such as the "Dolphin" of Carmichael[12] and X-35 of Parsons, et al.[14] These are not considered here because they were developed for Reynolds numbers much lower than in the present study.

C. Drag Calculations at $R_{\forall} = 10^8$

This represents the case of large airships and small submarines. Carmichael's experiments at $R_{\forall} \sim 10^7$ indicate that the LBL can survive up to $X/L \sim 0.5$ on the body surface. There have been arguments about the LBL existence at higher Reynolds numbers for shorter, but not negligible, distances. Since this has not been demonstrated conclusively at this high $R_{\forall}$, the calculations were carried out with transition fixed at $X/L = 0.034$; however, transition calculations were done later to verify this assumption. For fixed transition at $X/L = 0.034$, the drag results of different profiles are also shown in Table 1. A rough comparison with the results of the calculation of Parsons and Goodson[2] is possible for body I-36 by using a Reynolds number correlation. Based on the simplified drag formula of Hess,[11] one can show that

$$C_{D1}/C_{D2} = (\log R_{L_2}/\log R_{L_1})^{2.58} \tag{10}$$

for a given profile with a TBL over most of the body. Thus, the value of $C_{D\forall} = 0.0128$ predicted by our scheme at $R_{\forall} = 10^8$, corresponds to 0.0203 at $R_{\forall} = 5 \times 10^6$ compared to 0.02 reported by Parsons and Goodson. Similarly, for Myring's body, the value predicted herein at $R_{\forall} = 10^8 (R_L = 3.967 \times 10^8)$ corresponds to C_{DS} of 0.00328 at $R_L = 10^7$. This compares well with 0.00332 reported by Myring.

The results of Table 1 indicate that $C_{D\forall} \cong 0.013$ and is almost a constant for all bodies independent of the profile shape. Parsons and Goodson noticed similar behavior; however, Hess[11] showed a slow increase in $C_{D\forall}$ with the fineness ratio (for F.R. ≥ 3.0). A careful evaluation of the results of Table 1 may indicate the superiority of the laminar shapes for the following reasons:

1) For a given $R_{\forall}$, although the results do not suggest any substantial advantage of any of the profiles, the laminar shapes are expected to perform better. This is based on sustaining the LBL. Such existence is possible under conditions of low freestream turbulence, smooth surfaces, and negligible vibrations.

2) For applications with restriction on the frontal area, A, R_A $(= U_\infty \sqrt{A}/\nu)$ is fixed. Table 1 shows that R_A does not vary much and the turbulent profiles have substantially higher C_{DA} compared to the laminar shapes. If we want to be more exact, the effect of the variation of R_A on C_{DA} can be eliminated by using a Reynolds number drag correlation such as Eq. (10). However, this showed no significant change and

bodies F-57 and F2-49 still have the lowest C_{DA} by a wide margin.

3) Table 1 indicates that R_L is lower for laminar shapes. If Eq. (10) is used to calculate drag coefficients at a fixed R_L, the laminar profile drag coefficients will be reduced and their advantage becomes more obvious.

So it appears that bodies F2-49 and F-57 are the best for applications with specified R_A or R_L, while the best profile for applications of fixed $R_\forall$ will depend on the transition characteristics of each body.

To verify the assumption of complete TBL, transition calculations were carried out. After the two empirical transition criteria (discussed in Sec. III) were incorporated in the program, a relatively recent paper on the subject by Granville[35] was broght to our attention. Granville clearly showed (in Fig. 2 of Ref. 35) that among the two-dimensional methods, the Crabtree criterion gives better agreement over a wider range of $(\theta^2/\nu)(dU/ds)$ compared to other methods. For example, the van Driest and Blumer method[31] behaves very poorly where dU/ds is positive. Therefore, the van Driest and Blumer method has been discarded. Granville developed a new criterion specifically for axisymmetric bodies. Since more experimental data are required to assess the value of the new criterion as expressed in the discussion following Granville's paper, we decided to continue our calculations with the Crabtree criterion for the present time. It should be noted that transition prediction is the most uncertain part in the drag package. However, this should not undermine the present results since the study is comparative, i.e., the values of the calculated drag coefficients may not be physically accurate if the transition location is to be predicted. In spite of this, the ranking of different profiles from the drag point of view is quite good.

A transition study at $R_\forall = 10^8$ for the eight bodies is shown in Figs. 5a and 5b and the results are given in Table 2. It appears that the assumption of $(X/L)_{tr} = 0.03$ was not a bad one, since for most of the bodies $(X/L)_{tr} \leq 0.06$. Only the Tunny and F2-49 gave $(X/L)_{tr} \simeq 0.07$. To keep the boundary-layer laminar at this high Reynolds number, a strong flow acceleration is required; this means relatively thick bodies. However, the maximum thickness is limited by the possibility of separation. The other alternatives are to move the location of the maximum thickness forward and carefully redesign the nose shape. The use of the inverse problem seems attractive to design such a body shape by assuming a velocity distribution with the peak closer to the leading stagnation point. This technique is currently under investigation.

D. Drag Calculations at $R_\forall = 5 \times 10^7$

This Reynolds number represents the case of small airships and large torpedoes. The existence of a considerable laminar portion of the boundary layer is more feasible compared to the previous case. Therefore, the transition location was calculated, not assumed, using the Crabtree method and again the results should be quite good on a comparative basis.

The transition characteristics of different profiles are shown in Figs. 6a and 6b, while transition locations are given in Table 3. It is clear that transition is triggered for all turbulent bodies (Fig. 6b) and the Tunny, Dolphin, and F2-49 among the laminar bodies (Fig. 6a) quite early. The early transition for body F2-49 represents a major discrepancy with the Parsons and Goodson results. They reported a transition location $(X/L)_{tr}$ of 0.46 and a value of 0.0073 for the drag coefficient $C_{D\forall}$. Our calculations gave $(X/L)_{tr} = 0.076$ and a corresponding value of 0.0144 for $C_{D\forall}$. We feel that the present results are more realistic, since the upper limit for the applicability of Michel's and the e^9 transition criteria used by Parsons and Goodson has been exceeded. Cebeci, et al.[19] reported that Michel's criterion should be used within the range $R_s = 0.4 \times 10^6$ to 7×10^6 and the Smith-Gamberoni e^9 (Ref. 36) correlation within the range $R_s = 0.1 \times 10^6$ to 60×10^6. However, Smith and Gamberoni recommend the range $0.3 \times 10^6 \leq R_s \leq 20 \times 10^6$ for their correlation. This appears to be more reasonable, since no experimental data were found beyond $R_s = 17 \times 10^6$ in their correlation between measurement and prediction by stability theory. On the other hand, the Parsons and Goodson results indicate that R_s ranges from 21.7×10^6-10^8 for X/L between 0.1 and 0.46 for this body (F2-49).

As for the Shark and F-57 profiles, no transition is indicated within the limits of Fig. 6b. However, the curve of body F-57 comes very close to the Crabtree transition curve in the range $R_\theta = 1600$-2000 in contrast with the Shark curve. Since the uncertainty in the correlation curve is not negligible (a characteristic of all transition criteria), it is conceivable that transition may be triggered for body F-57 in this range—say at $X/L \cong 0.1$ where the two curves approach one another. The corresponding drag coefficient $C_{D\forall}$ is 0.0141 (Fig. 10). This is about the same for all other bodies with the exception of the Shark whose advantage becomes undisputed. However, if the

Table 2 Summary of the transition results (Crabtree method)—$R_\forall = 10^8$

Body	Tunny	Dolphin	Shark	F-57	F2-49	Myring	I-36	4165
$(R_\theta)_{tr}$	2300	1600	1300	1750	2140	2180	2300	2100
$(X/L)_{tr}$	0.0726	0.0300	0.0401	0.0475	0.0667	0.0595	0.0600	0.0481

Table 3 Summary of the results at $R_\forall = 5 \times 10^7$

Body	Tunny	Dolphin	Shark	F-57	F2-49	Myring	I-36	4165
$10^{-8} R_L$	1.8288	2.2646	1.8245	1.8743	1.6096	1.9835	2.3178	2.3529
$10^{-8} R_A$	0.3500	0.3492	0.3492	0.3886	0.4075	0.3164	0.3245	0.2979
$(R_\theta)_{tr}$	1930	1460	3080	1800 (3680)	1640	1790	2100	1880
$(X/L)_{tr}$	0.0987	0.0492	0.3689	0.104 (0.4222)	0.0758	0.0777	0.0965	0.0744
$C_{D\forall}$	0.0139	0.0143	0.0114	0.0141 (0.0086)	0.0144	0.0140	0.0135	0.0141
C_{DA}	0.0284	0.0293	0.0234	0.0233 (0.0142)	0.0217	0.0350	0.0320	0.0397
C_{DS}	0.0022	0.0021	0.0018	0.0023 (0.0014)	0.0024	0.0021	0.0019	0.0019

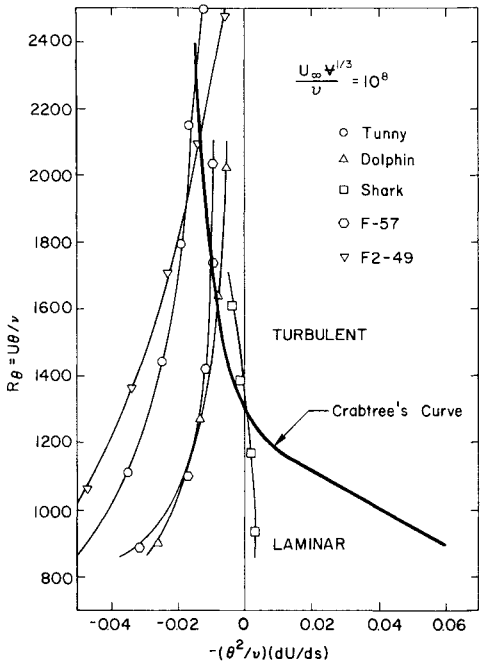

Fig. 5a Transition prediction for laminar profiles, $R_{\forall} = 10^8$.

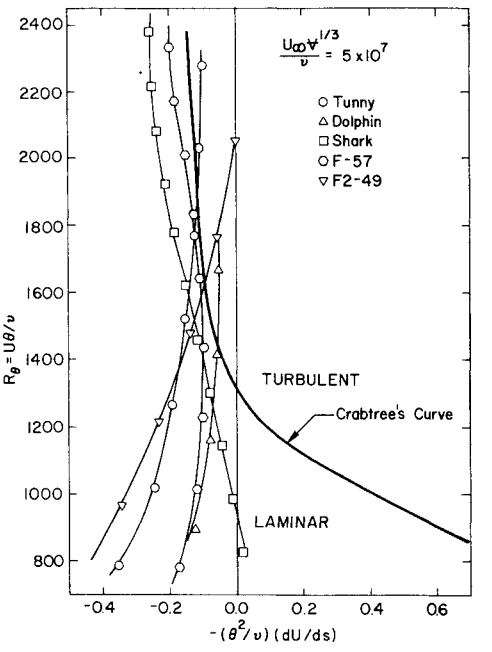

Fig. 6a Transition prediction for laminar profiles, $R_{\forall} = 5 \times 10^7$.

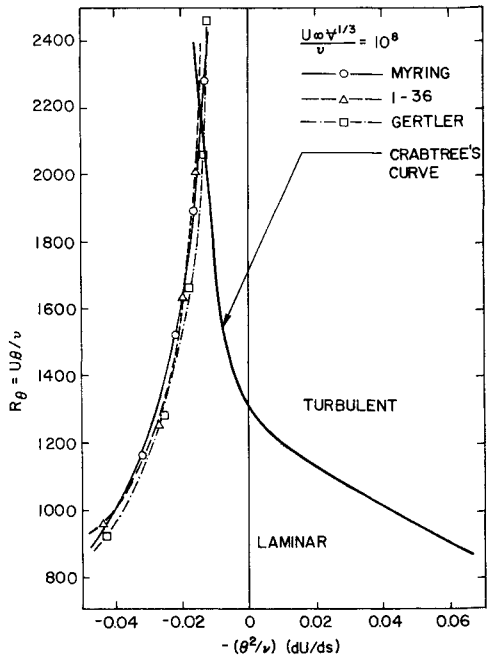

Fig. 5b Transition prediction for turbulent profiles, $R_{\forall} = 10^8$.

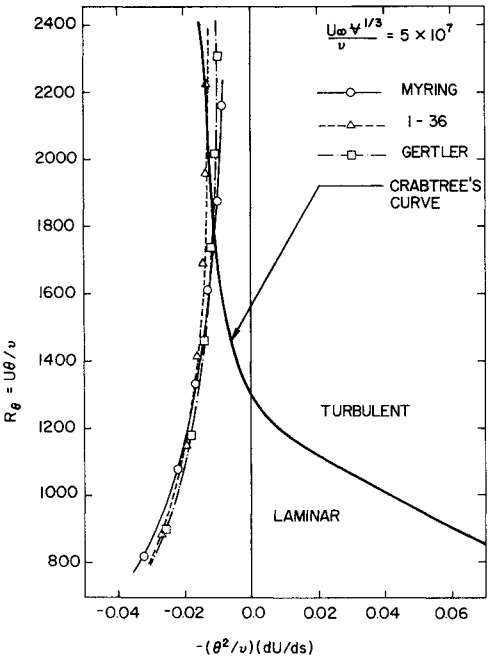

Fig. 6b Transition prediction for turbulent profiles, $R_{\forall} = 5 \times 10^7$.

F-57 profile succeeds in sustaining an LBL in the range $1600 \leq R_\theta \leq 2000$, then its transition characteristic becomes better than the Shark, as indicated by Fig. 7. If the Crabtree curve is extrapolated, as shown in Fig. 7 just for comparison purposes, the transition values of R_θ are 3680 and 3080 for the F-57 and Shark profiles, respectively. This corresponds to $(X/L)_{tr}$ of 0.422 (compared to 0.46 predicted by Parsons and Goodson) and $C_{D\forall}$ of 0.0086 for the F-57 and $(X/L)_{tr}$ of 0.369 and $C_{D\forall}$ of 0.0114 for the Shark. Thus, the body F-57 seems more attractive as a low-drag design for this Reynolds number if we can insure no transition in the range $0.08 \leq X/L \leq 0.13$. The inviscid flow velocity distribution of the two bodies is shown on Fig. 8. Notice that dU/ds is greater for the Shark in the range $0.07 \leq X/L \leq 0.25$ providing higher stability for the boundary layer as compared to the F-57 profile. So it appears that a slight modification in the velocity distribution of the F-57 profile to increase dU/ds and, consequently, the bondary-layer stability, can prevent transition in this range by offsetting the transition characteristic curve to the left on Fig. 7. A suggested modification in the velocity distribution is shown in Fig. 8. The inverse problem can be used to develop the modified body shape.

The boundary-layer development for these two bodies is described in Fig. 9 in terms of the variation of H and θ along the body. The solution for body F-57 is shown for the two transition locations discussed earlier. Figure 10 shows the corresponding variations of C_f and $C_{D\forall}(X)$. Notice the effect on the value of $C_{D\forall}$ of the F-57 profile for the two transition positions. It is worth noting that TBL separation is indicated at $X/L = 0.985$ for the Shark. This was neglected in the drag

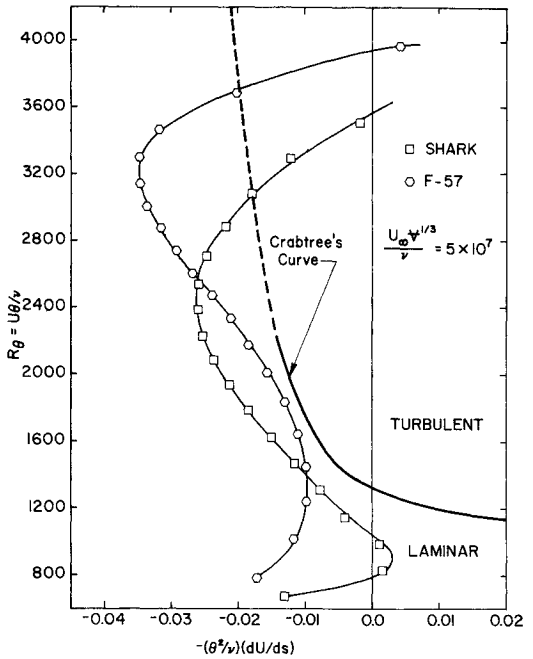

Fig. 7 Transition prediction for the Shark and F-57 bodies, $R_\forall = 5\times10^7$.

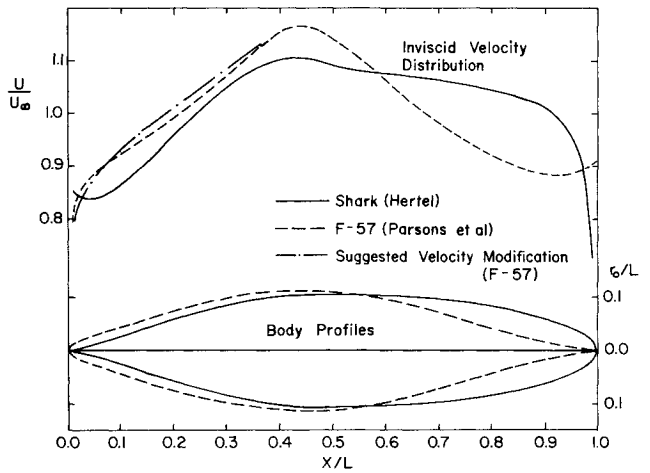

Fig. 8 Profile shapes and velocity distributions for the Shark and F-57 bodies.

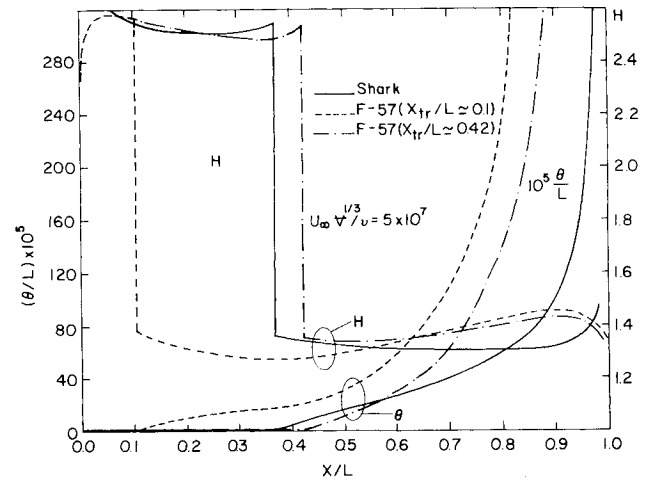

Fig. 9 Boundary-layer development for the Shark and F-57 bodies.

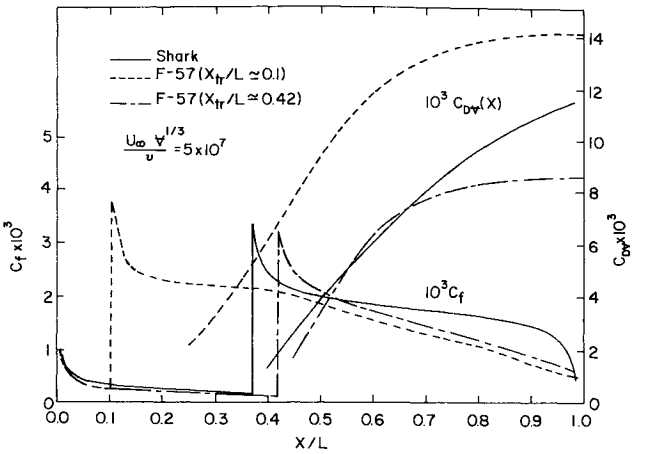

Fig. 10 Drag and skin friction coefficients prediction for the Shark and F-57 bodies.

calculations, since it is very close to the trailing stagnation point. Presumably some streamlining near the tail may be necessary to avoid such separation.

V. Summary and Conclusions

The drag characteristics of a number of the best available body shapes for high Reynolds number applications have been investigated using a numerical drag calculation scheme. The drag package has been demonstrated to predict the drag quite accurately by comparison to experimental data. The investigation was carried out at two Reynolds numbers ($R_\forall = 10^8$ and 5×10^7) representing flow around airships, small submarines, and large torpedoes. The results are summarized below.

At $R_\forall = 10^8$

a) The assumption of a TBL over most of the body surface appears to be quite correct for all investigated shapes. However, it is conceivable to expect a short run of LBL (say up to $X/L = 0.15$ or 0.2) by moving the maximum thickness forward and carefully designing the nose shape. This possibly may be achieved by solving the inverse problem for a velocity distribution with maximum velocity at $X/L \simeq 0.25$.

b) The drag coefficient $C_{D\forall}$ is about 0.013 for the different shapes and appears to be independent of both the hull shape and fineness ratio as long as the boundary layer is unseparated.

c) For a given $R_L (\sim 4\times10^8)$ or a given $R_A (\sim 6.5\times10^7)$, the F2-49 and F-57 laminar profiles have the lowest drag among all investigated shapes, even with the assumption of the boundary layer being turbulent over 97% of the body.

At $R_\forall = 5\times10^7$

a) Transition calculations based on Crabtree's method indicated that the F2-49 profile is not an optimum or even suboptimum shape for this Reynolds number. All bodies, with the exception of the Shark and F-57, have transition within the first 10% of the body length and about the same drag coefficient $C_{D\forall} (\simeq 0.014)$.

b) The transition characteristic curve of the F-57 comes very close to the Crabtree curve in the range $1600 \le R_\theta \le 2000$ which corresponds to about $0.08 \le X/L \le 0.13$. If transition is triggered in this region, the Shark shape will give the lowest $C_{D\forall}$. However, if the LBL can survive in this region, the F-57 will have transition at X/L quite after that of the Shark and, consequently, will have lower $C_{D\forall}$.

c) The danger of early transition for the F-57 body can be prevented by slightly changing the velocity distribution in the range $0.05 \le X/L \le 0.35$ to increase dU/ds for $X/L < 0.17$.

The inverse problem can then be used to find the corresponding change in the body shape. This is currently under investigation.

Acknowledgments

The authors would like to express their appreciation to V. C. Patel of the University of Iowa for providing them with his thick axisymmetric TBL program and to J. Hess of the Douglas Aircraft Company for providing the Douglas potential flow program for bodies of revolution.

References

[1] Huang, C. J. and Dalton, C., "Cargo Transportation by Airships: A Systems Study," NASA CR-2636, 1976.

[2] Parsons, J. S. and Goodson, R. E., "The Optimum Shaping of Axisymmetric Bodies for Minimum Drag in Incompressible Flow," Purdue University Rept. ACC-72-6, June 1972.

[3] Bristow, D. R., "A Solution to the Inverse Problem for Incompressible Axisymmetric Potential Flow," Paper presented at the AIAA Fluid Dynamics Conference, Palo Alto, Calif., June 1974.

[4] Zedan, M. F. and Dalton, C., "Incompressible Irrotational Axisymmetric Flow about a Body of Revolution: The Inverse Problem," *Journal of Hydronautics*, Vol. 12, Jan. 1978, pp. 41-47.

[5] Zedan, M. F. and Dalton, C., "Potential Flow around Axisymmetric Bodies: Direct and Inverse Problems," *AIAA Journal*, Vol. 16, March 1978, pp. 242-251.

[6] Gertler, M., " Resistance Experiments on a Systematic Series of Streamlined Bodies of Revolution—For Application to the Design of High-Speed Submarines," Rept. C-849, David Taylor Model Basin, Naval Ship Research & Development Center, Washington, D. C., 1950.

[7] Cebeci, T. and Bradshaw, P., *Momentum Transfer in Boundary Layers*, McGraw-Hill Book Co., Inc., New York, 1977.

[8] Patel. V. C., "A Simple Integral Method for the Calculation of Thick Axisymmetric Turbulent Boundary Layers," *Aeronautical Quarterly*, Vol. 25, 1974, p. 47.

[9] Crabtree, L. F., "Prediction of Transition in the Boundary Layer on an Aerofoil," *Journal of Royal Aeronautical Society*, Vol. 62, 1958, p. 525.

[10] Nakayama, A. and Patel, V. C., "Calculation of the Viscous Resistance of Bodies of Revlolution," *Journal of Hydronautics*, Vol. 8, Oct. 1974, pp. 154-163.

[11] Hess, J. L., "On the Problem of Shaping an Axisymmetric Body to Obtain Low Drag at Large Reynolds Numbers," *Journal of Ship Research*, Vol. 20, 1976, p. 51.

[12] Carmichael, B. H., "Underwater Drag Reduction Through Optimal Shape," *Underwater Missile Propulsion*, L. Greiner, (ed.), Compass Publications, Inc., Arlington, Va., 1966.

[13] Hertel, H., "Full Integration of VTOL Power Plants in the Aricraft Fuselage," *Gas Turbines*, AGARD CP No. 9, Pt. 1, 1966.

[14] Parsons, J. S., Goodson, R. E., and Goldschmied, F. R., "Shaping of Axisymmetric Bodies for Minimum Drag in Incompressible Flow," *Journal of Hydronautics*, Vol. 8, July 1974, pp. 100-107.

[15] Myring, D. F., " A Theoretical Study of Body Drag in Subcritical Axisymmetric Flow," *Aeronautical Quarterly*, Vol. 28, 1976, p. 186.

[16] Young, A. D., "The Calculation of Total and Skin Friction Drags of Bodies of Revolution at Zero Incidence," Aeronautical Research Council, R & M 1874, April 1939.

[17] Cebeci, T. and Smith, A. M. O., "Remarks on Methods of Predicting Viscous Drag," Paper 124, AGARD Conference on Aerodynamic Drag, Izmir, Turkey, April 1973.

[18] Granville, P., "The Calculation of Viscous Drag of Bodies of Revolution," Rept. 849, David Taylor Model Basin, Washington, D. C., 1953.

[19] Cebeci, T., Mosinskis, G. J., and Smith, A. M. O., "Calculation of Viscous Drag and Turbulent Boundary Layer Separation on Two-Dimensional and Axisymmetric Bodies in Incompressible Flows," Douglas Aricraft Co. Rept. MDC-J0973-01, Nov. 1970.

[20] Schlichting, H., *Boundary Layer Theory*, McGraw-Hill Book Co., Inc., New York, 1968.

[21] Hess, J. L. and Smith, A. M. O., "Calculation of Potential Flow About Arbitrary Bodies," *Progress in Aeronautical Sciences*, Vol. 8, Pergamon Press, 1967.

[22] Cebeci, T., Mosinskis, G. J., Smith, A. M. O., "Calculation of Viscous Drag in Incompressible Flows," *Journal of Aircraft*, Vol. 9, 1972, pp. 691-693.

[23] Smith, A. M. O. and Pierce, J., "Exact Solution of the Neumann Problem," Douglas Rept. ES26988, Douglas Aircraft Co., Long Beach, Calif., April 1958.

[24] Cebeci, T., Smith, A. M. O., and Wang, L. C., "A Finite-Difference Method for Calculating Compressible Laminar and Turbulent Boundary Layers," Rept. DAC-67131, Douglas Aircraft Co., Long Beach, Calif., March 1969.

[25] Truckenbrodt, E., "A Method of Quadrature for Calculation of Laminar and Turbulent Boundary Layers in Case of Plane and Rotationally Symmetric Flow," NACA TM 1379, May 1955.

[26] Rott, N. and Crabtree, L. F., "Simplified Laminar Boundary-Layer Calculations for Bodies of Revolution and for Yawed Wings," *Journal of Aeronautical Science*, Vol. 19, 1952, p. 553.

[27] Cebeci, T. and Smith, A. M. O., *Analysis of Turbulent Boundary Layers*, Academic Press, New York, 1974.

[28] Patel. V. C., "On the Equations of a Thick Axisymmetric Turbulent Boundary Layer," Rept. 143, Iowa Institute of Hydraulic Research, Iowa City, Iowa, 1973.

[29] Patel. V. C., Nakayama, A., and Damian, R., "Measurements in the Thick Axisymmetric Turbulent Boundary Layer Near the Tail of a Body of Revolution." *Journal of Fluid Mechanics*, Vol. 63, 1974, p. 345.

[30]. Thompson, B. G. J., "A New Two-Parameter Family of Mean Velocity Profiles for Incompressible Turbulent Boundary Layers on Smooth Walls," Aeronautical Research Council R & M 3463, London, 1965.

[31] van Driest, E.R. and Blumer, C.B., "Boundary Layer Transition: Freestream Turbulence and Pressure Gradient Effects," *AIAA Journal*, Vol. 1, June 1963, pp. 1303-1306.

[32] Zedan, M. F., Ph.D. Thesis, University of Houston, Houston, Texas, 1979.

[33] Nash, J. F., "Turbulent Boundary Layer Behavior and the Auxiliary Equation," Aeronautical Research Council CP 835, London, 1965.

[34] Nash, J. F., "A Note on Skin-Friction Laws for the Incompressible Turbulent Boundary Layer," NPL Aero. Report 1135, 1964.

[35] Granville, P. S., "The Prediction of Transition from Laminar to Turbulent Flow in Boundary Layers on Bodies of Revolution," *Tenth Symposium Naval Hydrodynamics*, R. D. Cooper and S. W. Doroff (Eds.), U.S. Government Printing Office, Washington, D.C., 1974, pp. 705-729.

[36] Smith, A. M. O. and Gamberoni, N., "Transition, Pressure Gradient, and Stability Theory," Douglas Aircraft Co. Rept. ES26388, Aug. 1956.